Oncogene 35.23 (2016): 2991-3003

DOI: 10.1038/onc.2015.366

SPROUTY-2 represses the epithelial phenotype of colon carcinoma cells via upregulation of ZEB1 mediated by ETS1 and *miR-200*/*miR-150*

Antonio Barbáchano[1], Asunción Fernández-Barral[1#], Fábio Pereira[1#], Miguel F. Segura[2,†], Paloma Ordóñez-Morán[1,§], Enrique Carrillo-de Santa Pau[4], José Manuel González-Sancho[1], Douglas Hanniford[2], Natalia Martínez[3], Alba Costales-Carrera[1], Francisco X. Real[4,5], Héctor G. Pálmer[6], José María Rojas[3], Eva Hernando[2], and Alberto Muñoz[1]

[1] Instituto de Investigaciones Biomédicas "Alberto Sols", Consejo Superior de Investigaciones Científicas, Universidad Autónoma de Madrid, E-28029 Madrid, Spain; [2] Department of Pathology, New York University School of Medicine, NY10016, USA; [3] Unidad de Biología Celular, Unidad Funcional de Investigación en Enfermedades Crónicas, Instituto de Salud Carlos III, E-28220 Majadahonda, Madrid, Spain; [4] Centro Nacional de Investigaciones Oncológicas, E-28029 Madrid, Spain; [5] Universitat Pompeu Fabra, E-08003 Barcelona, Spain; [6] Vall d'Hebron Institute of Oncology, E-08035 Barcelona, Spain

[†] Present address: Vall d'Hebron Institut de Recerca (VHIR), E-08035 Barcelona, Spain

[§] Present address: Cancer Stem Cell Laboratory, École Polytechnique Fédérale de Lausanne, CH-1015 Lausanne, Switzerland

[#] Both authors contributed equally to this manuscript

*Correspondence:
Instituto de Investigaciones Biomédicas "Alberto Sols", Arturo Duperier, 4, 28029 Madrid, Spain. Telephone: #34-91-5854451; Fax: #34-91-5854401. E-mail: amunoz@iib.uam.es

Running title: SPROUTY-2 induces ZEB1 and EMT in colon cancer cells

ABSTRACT

SPROUTY-2 (SPRY2) is a modulator of tyrosine kinase receptor signaling with receptor- and cell type-dependent inhibitory or enhancing effects. Studies on the action of SPRY2 in major cancers are conflicting and its role remains unclear. Here we have dissected SPRY2 action in human colon cancer. Global transcriptomic analyses show that SPRY2 downregulates genes encoding tight junction proteins such as claudin-7 and occludin and other cell-to-cell and cell-to-matrix adhesion molecules in human SW480-ADH colon carcinoma cells. Moreover, SPRY2 represses *LLGLL2/HUGL2*, *PATJ1/INADL* and *ST14*, main regulators of the polarized epithelial phenotype, and *ESRP1*, an epithelial-to-mesenchymal transition (EMT) inhibitor. A key action of SPRY2 is the upregulation of the major EMT inducer ZEB1, as these effects are reversed by *ZEB1* knock-down by means of RNA interference. Consistently, we found an inverse correlation between the expression level of claudin-7 and those of SPRY2 and ZEB1 in human colon tumors. Mechanistically, ZEB1 upregulation by SPRY2 results from the combined induction of ETS1 transcription factor and the repression of microRNAs (*miR-200* family, *miR-150*) that target *ZEB1* RNA. Moreover, SPRY2 increased AKT activation by epidermal growth factor (EGF) whereas AKT and also Src inhibition reduced the induction of ZEB1. Altogether, these data suggest that AKT and Src are implicated in SPRY2 action. Collectively, these results show a tumorigenic role of SPRY2 in colon cancer that is based on the dysregulation of tight junction and epithelial polarity master genes via upregulation of ZEB1. The dissection of the mechanism of action of SPRY2 in colon cancer cells is important to understand the upregulation of this gene in a subset of patients with this neoplasia that have poor prognosis.

Keywords: SPROUTY-2, colon cancer, ZEB1, AKT, ETS1, claudin-7

INTRODUCTION

SPROUTY-2 (SPRY2) belongs to a family of intracellular modulators of tyrosine kinase receptor signaling.[1,2] SPRY2 action is receptor- and cell type-dependent: it inhibits signaling by activated fibroblast growth factor receptor (FGFR) and vascular endothelial growth factor receptor (VEGF) whereas it increases signaling by epidermal growth factor receptor (EGFR) in some cell types.[3,4] The underlying mechanisms include the inhibition of EGFR ubiquitination-dependent degradation and trafficking from early to late endosomes.[5,6]

Given the important role of EGFR and FGFRs on the biology of many epithelial cell types and as therapeutic targets in carcinomas and other cancers, SPRY2 is drawing increasing attention. However, the role of SPRY2 in cancer remains unclear.[2] In colon cancer, we have previously reported SPRY2 upregulation in high-grade tumors and at the invasion front of low-grade tumors.[7] Likewise, *SPRY2* RNA and protein levels are higher in colon adenocarcinomas than in normal adjacent mucosa.[8] In SW480-ADH colon cancer cells SPRY2 represses *CDH1*/E-cadherin and counteracts the adhesive phenotype induced by 1α,25-dihydroxyvitamin D_3.[7] Moreover, in HT-29 and LS-174T cells SPRY2 increases the level of c-MET and HGF-stimulated ERK and AKT phosphorylation, promoting cell migration and invasion.[8] Further supporting a tumorigenic role, *SPRY2* is upregulated in *KRAS* mutant colorectal cancer,[9] and in melanoma cells harbouring *N-RAS* or *B-RAF* mutations.[10,11] RNA expression repository databases show upregulation of SPRY2 expression in colorectal tumors versus others neoplasias.[12] Consistently, we have recently shown that *SPRY2* is a target of β-catenin/FOXO3a, a marker of poor prognosis in colon cancer.[13] In contrast, lower levels of *SPRY2* RNA have been reported in tumor *versus* normal tissue and in stage III/IV *versus* stage II colon cancer patients, as well as inhibitory effects of exogenous *SPRY2*

overexpression on the proliferation, migration and tumorigenic potential of HCT116 colon cancer cells xenografted in immunodeficient mice.[14] Also, SPRY2 appears to have tumor suppressive effects in breast, prostate, and liver cancers and in B-cell diffuse lymphoma.[15-19] These opposite effects are indicative of cell-type-dependent activities of SPRY2.[2]

To dissect the action of SPRY2 in colon cancer, we analyzed its effects on gene expression and phenotype of SW480-ADH cells. Transcriptomic analyses revealed the repression by SPRY2 of genes encoding proteins involved in cell-to-cell and cell-to-matrix adhesion or regulating epithelial cell polarity such as *ST14*, which codes for the membrane-anchored serine protease matriptase that is essential for the integrity of the intestinal epithelial barrier.[20] We show that most of the gene regulatory effects of SPRY2 are mediated by ZEB1, a major epithelial-to-mesenchymal transition (EMT) inducer. Thus, SPRY2 is a potent inhibitor of the epithelial phenotype in colon carcinoma cells by repressing tight junction and polarity regulators through the upregulation of *ZEB1*, which in turn results from the induction of the transcription factor ETS1 and the downregulation of micro(mi)RNAs (*miR200* family, *miR-150*) that target *ZEB1* RNA.

RESULTS

SPRY2 represses epithelial adhesion and polarity genes

To characterize the effects and dissect the mechanism of action of SPRY2 in colon carcinoma cells we generated SW480-ADH cells (containing low level of endogenous SPRY2 protein) stably expressing a wild type (AU5-tagged) SPRY2 (SPRY2-wt cells). We also generated cells expressing mutant S112A (SPRY2-S112A cells) or Y55F (SPRY2-Y55F cells) SPRY2 proteins, which respectively lack the phosphorylation site for Mnk1/2 kinases (Ser^{112}) or a tyrosine residue (Tyr^{55}) thought to be required for the interaction with c-Cbl and thus for potentiation of EGFR stability as well as for full FGF inhibitory activity.[21-24] Empty vector transfected cells (Mock) were used as control. All cell types had a similar polygonal morphology except SPRY2-Y55F cells that appeared more elongated (Figure 1a, left). Expression of exogenous SPRY2 proteins was confirmed by Western blot (Figure 1a, right).

To get insight into the mechanisms through which SPRY2 impacts on gene expression, we carried out a global transcriptomic analysis of the four transfectants. High correlation was observed between replicates (Supplementary Table 1), while SPRY2-wt and SPRY2-S112A have the lowest correlations between conditions. Samples were unambiguously clusterized by transfected type in a Principal Component Analysis (PCA) explaining most of the variance (99,7%) (Supplementary Figure S1). Furthermore, Single Enrichment Analysis (SEA) with differentially expressed transcripts (Supplementary Table 2) showed that genes related with cell-to-cell and cell-to-matrix adhesion were highly represented in the comparisons except for Mock *vs* SPRY2-S112A (Supplementary Table 3). These findings were also supported by a Gene Set Enrichment Analysis (GSEA) on adhesion-related KEGG and GO pathways (Figure 2). Our previous studies showed the capacity of SPRY2 to inhibit the expression of

CDH1/E-cadherin causing loss of intercellular adhesion.[7] Additionally, SPRY2 is preferentially expressed in cells at invasion front of human colon tumors *in vivo*.[7] These results, together with data from *in silico* analyses, led us to perform a detailed inspection of genes related to adhesion structures and pathways.

As compared to Mock cells, SPRY2-wt cells showed lower expression levels of genes encoding *adherens junctions* proteins (*CDH1*, *CDH3*), tight junctions proteins (*CLDN7*/claudin-7, *OCLN*/occludin) and other adhesion molecules (*GJB2*, *NCAM, JUP/CTNNG*) (Supplementary Table 2). Conversely, SPRY2-wt cells expressed higher level of *ZEB1* and *CLDN1*/claudin-1, which has been proposed to be protumorigenic in colon cancer.[25] SPRY2-wt cells showed also reduced expression of several genes encoding integrins (*ITGB8*, *ITGB4*, *ITGB2*, *ITGB6*) and extracellular matrix proteins (*TNC*, *LAMB3*, *LAMC2*, *LAMA3*). Downregulation of *CLDN7* and *OCLN* and upregulation of *CLDN1* and *ZEB1* in SPRY2-wt and SPRY2-Y55F cells were validated by qRT-PCR and Western blot (Figures 1b and c), using the reported inhibition of *CDH1*/E-cadherin as control.[7] GSEA revealed that the expression profiles of genes encoding adhesion and extracellular matrix proteins were significantly enriched in SPRY2-S112A cells and Mock cells compared to SPRY2-wt (Figure 2).

Further supporting a role of SPRY2 disrupting tight junction functionality and cell polarity, our transcriptomic study showed also reduced expression in SPRY2-wt and SPRY2-Y55 cells of *LLGL2/HUGL2*, *INADL/PATJ1* and *ST14*, polarity genes that promote tight junction formation and function as tumor suppressors (Supplementary Table 2 and Figures 1d and e).[20,26-28] SPRY2 represses also *Epithelial Cell Adhesion Molecule* (*EPCAM*) gene that is mutated in a proportion of Hereditary Non-Polyposis Colorectal Cancer patients and whose overexpression has tumor type-dependent effects on patient survival (Figures 1d and e).[29] EpCAM protein binds claudin-1 and claudin-7

and regulates their dynamics and the function of tight junctions.[30,31]. *Epithelial Splicing Regulatory Protein 1* (*ESRP1*), which encodes a broad splicing regulator in epithelial cells that prevents the EMT process,[32,33] was strongly downregulated in SPRY2-wt cells and, conversely, upregulated in SPRY2-S112A cells (Figure 1d). Consistent with the findings described above, the expression levels of ZEB1 and SPRY2 proteins directly correlate in a panel of colon carcinoma cell lines (Supplementary Figure S2). Collectively, these results indicate that SPRY2 ectopic expression causes loss of the epithelial phenotype (adhesiveness and polarity) by controlling multiple genes, and highlight the importance of Ser^{112} for this function.

To investigate how SPRY2 regulates tight junction genes, we cloned a fragment of *CLDN7* proximal promoter (-1136/+428 bp) upstream the luciferase reporter gene. Overexpression of SPRY2 markedly reduced the activity of *CLDN7* promoter (Figure 1f). ZEB1 is a major inducer of EMT that represses a number of epithelial adhesion genes. We found an inverse relation between the expression level of claudin-7 and ZEB1 proteins in the four cell types (Figure 1c). Interestingly, ectopic expression of ZEB1 inhibited *CLDN7* promoter in Mock cells but did not further decrease its activity in SPRY2-wt cells, which is consistent with the high level of ZEB1 expression in the latter cells (Figure 1f). This supports a major role of ZEB1 in the repression of *CLDN7* by SPRY2.

ZEB1 mediates the repression of epithelial adhesion and polarity genes by SPRY2

Given that *ESRP1*, *LLGL2/HUGL2* and *ST14* genes are repressed by ZEB1 in other systems,[34-36] we sought to elucidate to what extent the gene regulatory effects of SPRY2 depend on ZEB1. We knock-downed *ZEB1* by transfection of shRNA in Mock cells, as confirmed at the RNA and protein levels (Figures 3a and b). *ZEB1* downregulation

increased *CDH1, CLDN7, ST14, OCLDN*, and *ESRP1* RNA (Figure 3a). Data on claudin-7, E-cadherin, ST14 and EpCAM were reproduced at the protein level (Figure 3b). In agreement with the reciprocal negative feedback loop of regulation described in other systems,[37-39] ZEB1 knock-down caused the upregulation of *miR-200b* and *miR-200c* (Figure 3c). Similar results were obtained in SPRY2-wt cells in which ZEB1 was silenced by lentivirus transduction of *ZEB1* shRNA (Figures 3d-f). Moreover, interference expression of *ZEB1* in SPRY2-wt cells induced *CLDN7* and *CDH1* promoters (Figure 3g). Identical results were obtained by using lentiviruses to knock-down ZEB1 expression in Mock cells (Supplementary Figure S3). These results strongly suggest that ZEB1 mediates the dysregulation of tight junction and epithelial polarity genes by SPRY2 and that ZEB1 is a probable direct repressor of claudin-7.

Inverse correlation between the expression of SPRY2 and ZEB1 with that of claudin-7 in colon tumors

To explore the relevance of these findings *in vivo*, we analyzed the expression of SPRY2, ZEB1 and claudin-7 in tissue microarrays of tumors of colon cancer patients (Figure 4a). Significant positive correlation between the expression of SPRY2 and ZEB1 ($n = 39$, $r = 0.63$, $P < 0.0001$) and negative correlation between that of ZEB1 and claudin-7 ($n = 53$, $r = -0.36$, $P = 0.007$) and SPRY2 and claudin-7 ($n = 34$, $r = -0.35$, $P = 0.037$) were found (Figure 4b). These results were consistent with those obtained in cultured cells supporting the idea that the regulation of ZEB1 by SPRY2 and the repression of claudin-7 by ZEB1 occur also *in vivo* in human colon tumors.

Mechanism of ZEB1 upregulation by SPRY2

To investigate the mechanism of *ZEB1* upregulation by SPRY2 we first studied whether this effect could be mediated by the modulation of *miRs* targeting *ZEB1* RNA. An *in silico* analysis of *ZEB1*-RNA-3'UTR region using three independent target prediction algorithms (TargetScan, miRANDA, PicTar) revealed the presence of several putative binding sites for evolutionarily conserved *miR* species: *miR-142-3p, miR-23, miR-150, miR-342-3p* and the previously described *miR-200b/c* [37-39] (Figure 5a). To examine the role of these miRs in *ZEB1* RNA regulation by SPRY2, their expression was analyzed by qRT-PCR in Mock and SPRY2-wt cells. *miR-142-3p, miR-23a* and *miR-150,* and also *miR-200b, miR-200c*, but no *miR-342-3p,* were expressed at lower level in SPRY2-wt cells than in Mock cells (Figure 5b). Reduced expression of *miR-200b* and *miR-200c* was also detected in SPRY2-Y55F cells, but not in SPRY2-S112A cells (Figure 5c).

To determine whether these miRNAs directly modulate *ZEB1* levels, we cloned a fragment of *ZEB1*-RNA-3'UTR containing the putative miRNA-binding sites into the psiCHECK2 dual luciferase reporter vector. Co-transfection of HEK293T cells with mimic oligonucleotides of *miR-200b, miR-142-3p and miR-150,* but not *miR-23a,* together with a *ZEB1*-RNA-3'UTR-luciferase construct, resulted in reduced luciferase activity at both low (5 nM) and high (50 nM) amount of transfected oligonucleotides (Figure 5d). Moreover, mutation of predicted binding sites for *miR-200* family and *miR-150,* but not for *miR-142-3p* (Figure 5e, left), reverted this effect, indicating that *miR-200* and *miR-150* are direct modulators of ZEB1 (Figure 5e, right). Transfection of *miR-200b* into SPRY2-wt cells reduced the expression of *ZEB1* RNA and protein more efficiently than the transfection of *miR-150 or miR-142-3p* using scrambled-transfected SPRY2-wt cells and Mock cells as controls (Figures 5f and g). Consistently, only *miR-200b* led to upregulation of claudin-7 and E-cadherin (Figure 5g). These results show a

preferential regulation of *ZEB1* RNA by *miR-200* and an additional effect of *miR-150*, and support that the repression of claudin-7 by SPRY2 is mediated by ZEB1.

To examine whether SPRY2 could control directly the expression of *miR-200b/c*, we used luciferase-reporter vectors containing the promoter of *miR-200b/a* (miR-200b-a-429 (-321/+120))[40] and *miR-200c* (hsa-miR-200c promoter (-683/-67)).[39] First, these plasmids were transfected into Mock and SPRY2-wt cells. A stronger reduction in the activity of *miR-200b/a* and *miR-200c* promoters was found in SPRY2-wt cells that express SPRY2 constitutively, while transfected ZEB1 expression vector further decreased the activity of the two promoters in Mock cells but not in SPRY2-wt cells (Figure 5h). Second, ZEB1 and SPRY2 expression vectors were transiently transfected in SW480-ADH cells. Exogenous SPRY2 did not change the activity of the two *miRs* promoters and did not affect their inhibition by ZEB1 (Figure 5i, left). These results agree with the reported direct inhibition of *miR-200b/a and miR-200c* promoters by ZEB1 and suggest that the effect of SPRY2 is mediated by the upregulation of *ZEB1*, which does not take place at sufficient level upon transient SPRY2 transfection (Figure 5i, right).

Next we studied putative mediators of the upregulation of ZEB1 by SPRY2. Given the relation between SPRY2 and EGF signaling[3,4] this pathway was chosen for detailed study. In concordance with other reports,[41] SPRY2-wt did not change the basal or EGF-induced levels of active (phosphorylated) ERK (Figure 6a), which may be related to the presence of a mutated *K-RAS* gene in SW480-ADH cells. By contrast, SPRY2 amplified the activation of AKT induced by EGF (Figure 6b). Additionally, reduction of active phospho(p)-AKT, using wortmannin (PI3K inhibitor) or MK2266 (AKT inhibitor) decreased the level of ZEB1 (Figure 6c). Likewise, the Src inhibitor PP2 decreased ZEB1 expression in Mock and SPRY2-wt cells and increased that of

claudin-7 in Mock cells (Figure 6d). Thus, AKT and Src seem to participate in the upregulation of ZEB1 by SPRY2.

ETS1 mediates the upregulation of ZEB1 by Snail1 in mouse breast epithelial cells,[42] and our transcriptomic analysis revealed that the RNA level of *ETS1* transcription factor is 1.62-fold higher in SPRY2-wt cells than in Mock cells, while no differences were found for *ETS2* (Supplementary Table 2). Therefore, we investigated its implication in SPRY2 action. First, we confirmed by Western blot analysis the presence of higher level of ETS1 protein in SPRY2-wt and SPRY2-Y55F cells than in Mock and SPRY2-S112A cells (Figure 6e). Second, transduction of SPRY2-wt cells with lentiviruses encoding *ETS1* shRNA led to a partial reduction of ZEB1 protein expression levels (Figure 6f). Third, in contrast, ETS1 expression was unaffected by ZEB1 knock-down in SPRY2-wt cells showing that no reciprocal regulation exists (Figure 6g). Fourth, overexpression of ETS1 by transient transfection of an exogenous cDNA increased ZEB1 expression (Figure 6h). These results suggest that ETS1 contributes to the induction of ZEB1 by SPRY2, which is most likely amplified by the repression of *miR-200* and *miR-150* species (Figure 6i).

DISCUSSION

This study shows that SPRY2 triggers a coordinated pattern of gene expression through the imbalance of the *ZEB1*/*miR200* switch in favor of ZEB1 upregulation mediated at least in part by ETS1 and AKT. This mechanism leads to the loss of polarized and adhesive epithelial phenotype.

Tight junctions are responsible for epithelial barrier function and polarity, and control cell proliferation and differentiation, which are disrupted at early and advanced stages of tumorigenesis.[43] In particular, downregulation of claudin-7 is an early event in colorectal cancer[44] and promotes tumorigenesis of colon cancer cells.[45,46] Data obtained in biopsies from colon cancer patients indicating an inverse relation between ZEB1 and claudin-7 expression are consistent with the downregulation of many tight junction and polarity genes by SPRY2 in SW480-ADH cells. In addition, they agree with the tumorigenic role of ZEB1 and its inverse relation between claudin-7 and other family members and ZEB1 in lung cancer.[47] Altogether, our results showing repression of tight junction proteins by SPRY2 strongly support a protumorigenic action in colon cancer.

Notably, mutation of Ser^{112} residue (SPRY2-S112A cells) abolishes most SPRY2 effects on the expression of epithelial genes. The role of this aminoacid in SPRY2 activity is controversial. One study has proposed that Ser^{112} phosphorylation by Mnk1, a kinase activated by p38MAPK, stabilizes Spry2 protein in Chinese hamster ovary (CHO)-K1 cells.[23] In contrast, another study shows that Mnk2 (also a p38MAPK substrate) but not Mnk1 phosphorylates SPRY2 leading to its association with the E3 ubiquitin ligase Nedd4 and posterior degradation in HEK293T cells.[24] Likewise, p38MAPK decreases Spry2 content in mouse embryo fibroblasts via phosphorylation of Siah2 E3 ubiquitin ligase.[48] Our results agree with this study as the p38MAPK inhibitor SB203080 increased the level of SPRY2 protein in Mock cells (not shown). In addition,

our data agree with those of Edwin *et al.* regarding the similar effects of wild-type and Tyr^{55} SPRY2 proteins.[24] Mutation of Tyr^{55}, that has been proposed to generate a dominant-negative SPRY2 in terms of inhibition of FGF signaling,[21-23] did not affect the repression of tight junction or polarity proteins (SPRY2-Y55F cells), indicating that this residue is important for only a subset of SPRY2 actions.

The precise mechanism by which SPRY2 regulates gene expression is not fully known. We analyzed the expression of the homeobox *SIX1* gene, which is overexpressed in colorectal cancer and promotes EMT at least in part via the repression of *miR-200* family and activation of *ZEB1*.[49] No differences were detected (Supplementary Figure S4). By contrast, the longer activation of AKT and the effect of AKT and Src inhibition on ZEB1 induction suggest that these two enzymes are implicated in SPRY2 action in SW480-ADH cells that, of note, overexpress EGF and harbor a mutated *K-RAS* gene. AKT and Src may contribute to upregulate ETS1, which in turn activates ZEB1.[42]

In conclusion, our findings support a key role of SPRY2 promoting the EMT process in colon carcinoma cells through ZEB1 induction by a mechanism that implies AKT/Src, ETS1 and *miR200/miR-150* species (Figure 6i). Why SPRY2 has, instead, tumor suppressor activity in other types of cancer cells remains to be elucidated.

MATERIALS AND METHODS

Cells and cell culture

Human colon carcinoma SW480-ADH and HEK293T embryonal kidney cell lines were cultured in RPMI and DMEM plus 10% fetal bovine serum respectively (Life technologies, Carlsbad, CA, USA). Cell lines were originally obtained from the American Type Culture Collection (ATCC) and authenticated using the *GenePrint*® 10 System (Promega, Madison, WI, USA), which allows co-amplification and three-color detection of ten human *loci*: TH01, TPOX, vWA, Amelogenin, CSF1PO, D16S539, D7S820, D13S317, D21S11 and D5S818. Short Tandem Repeat profiles were sent for comparison against cell line databases (ATCC, DSMZ). Last test was done in February 2014. SPRY2-wt, SPRY2-S112A and SPRY2-Y55F and Mock cells were generated by stable transfection of SW480-ADH cells with pCEFL-KZ-AU5, pCEFL-KZ-AU5-hSPRY2, pCEFL-KZ-AU5-hSPRY2 S112A or pCEFL-KZ-AU5-hSPRY2 Y55F plasmids.[50] Cells were tested routinely to ensure there was no mycoplasma contamination (Universal Mycoplasma Detection kit, ATCC, Manassas, VA, USA; #30-1012).

Antibodies and reagents

We used primary mouse monoclonal antibodies against E-cadherin (BD Transduction Laboratories, Franklin Lakes, NJ, USA; #610182), AU5 (Covance, Princeton, NJ, USA; MMS-135R), S6 ribosomal protein (Cell Signaling, Danvers, MA, USA; #23175) and p-ERK (Santa Cruz Biotechnology, Dallas, TX, USA; sc-7383); rabbit polyclonal antibodies against SPRY2 (Upstate, Billerica, MA, USA; #07-524), ETS1 and ERK 2 (Santa Cruz Biotechnology; sc-350 and sc-154 respectively), ZEB1 (Sigma-Aldrich, St Louis, MO, USA; #HPA027524), ST14 (Bethyl, Montgomery, TX, USA; A300-221A),

p-AKT (Ser473) (Cell Signaling; #9271), occludin, claudin-7 and claudin-1 (Life Technologies; #71-1500; #34-9100; #51-9000), EpCAM (Abcam, Cambridge, UK) and p-S6 ribosomal protein (Ser240/244) (Cell Signaling; #2215S); and goat polyclonal antibodies against ZEB1, AKT, β-actin and lamin B (Santa Cruz Biotechnology; sc-10572, sc1618, sc-1616 and sc-6216, respectively). HPR-conjugated secondary antibodies were anti-rabbit IgG (H+L) (Jackson Immunoresearch, West Grove, PA, USA; 111-035-045), anti-mouse IgG (H+L) (Promega; W402B) and anti-goat IgG (Santa Cruz Biotechnology; sc-2020). Secondary antibodies used for Odyssey Infrared Imaging were IRDye® 800 donkey anti-mouse IgG (H&L) (Rockland Inc, Gibertsville, PA, USA; #610-732-124) and IRDye® 680 donkey anti-rabbit IgG (Rockland Inc.; #926-32223). Inhibitors: Src-family tyrosine kinases, PP2 (Tocris, Bristol, UK, #1407); PI3K inhibitor, wortmannin (Cell Signaling; #99516), AKT inhibitor, MK2266 (Selleckchem, Munich, Germany; #S1078).

Cloning of *CLDN7*/claudin-7 promoter

A 1.56 kb fragment of the h*CLDN7*/Claudin-7 promoter (-1136/+428) similar to the one described by Kohno and colleagues[51] was amplified by PCR using human genomic DNA as template, and the following primers: forward 5'-GACAAGGAGTGAAACAGG-3' and reverse 5'-TTCCGCCCTCAGAAAACA-3'. The resulting product was cloned into the pGEM-T Easy vector (Promega) and sequenced. Subsequently, it was released with EcoRI, filled-in using the large fragment of *E. coli* DNA polymerase I (Klenow), and subcloned into the SmaI site of promoterless pGL3 basic *Firefly* luciferase expression vector (Promega).

Reporter assays

Reporter assays were performed in SW480-ADH, Mock, SPRY2-wt and HEK293T cells. Unless otherwise indicated, cells were transfected using the jetPEI reagent (PolyPlus Transfection, New York, NY, USA). *Firefly* (Luc) and *Renilla reniformis* luciferase (Rluc) activities were measured separately using the *GloMax*® 96 Microplate Luminometer (Promega). Luc activity was normalized to the Rluc activity (constitutive expression). The promoter constructs for *miR-200b/a* and *miR-200c* were generously provided by Prof. Gregory Goodall (Center for Cancer Biology, Adelaide, Australia) and Prof. Thomas Brabletz (University of Freiburg, Germany), respectively. pCDNA3-ZEB1 expression plasmid was provided by Dr. Antonio García de Herreros (Instituto Municipal de Investigación Médica, Barcelona, Spain). The results are represented as the average of the fold induction obtained from three independent experiments using quadruplicates.

3'-UTR Luciferase Assays: A portion of the *ZEB1*-RNA-3'UTR containing the studied putative miRNA binding sites was amplified by PCR using the primers forward 5'-*CTCGAG*CACAAAATAAATCCGGGTGTG-3' and reverse 5'-GCGGCCGCAGTCCCTGCAATCAGAACTCA-3', and cloned into psiCHECK2 luciferase reporter vector (Promega) using XhoI and NotI. HEK293T cells were seeded into 96-well plates (20 x 10^3 cells/well) and co-transfected (Lipofectamine 2000, Life technologies) with the *ZEB1*-RNA-3'UTR construct and the indicated amounts of mimic negative control (scrambled), *miR-200b*, *miR-142-3p*, *miR-23a* and *miR-150* miRIDIAN mimics (Dharmacon). Luciferase activity was measured 24 h later using the Dual-Glo Luciferase Assay System (Promega). Rluc activity was normalized to corresponding Luc activity and plotted as a percentage of the control. Mutations at the putative miRNA binding sites were generated using the QuickChange XL Site-Directed

Mutagenesis Kit (Stratagene, La Jolla, CA, USA) following the manufacturer's instructions. Luciferase assays were performed at least three times using triplicates.

RNA interference and overexpression strategies

ZEB1 knock-down in Mock cells was performed as described.[52] *ZEB1* silencing in SPRY2-wt and Mock cells, and *ETS1* silencing in SPRY2-wt cells was carried out using the lentiviral vector pGIPz containing different shRNA^{mir} sequences: *ZEB1*, V3LHS_356186 (sh1), V3LHS_356187 (sh2) and V2LHS_226625 (sh3); *ETS1*, V2LHS_244928 (sh1) and V3LHS_301171 (sh2) (Dharmacon, GE Healthcare, Pittsburgh, PA, USA). Non-silencing shRNA^{mir} sequence (NS), with no homology to known mammalian genes was used as control, cloned in pGIPz vector (Dharmacon). Lentiviruses were produced and tittered as previously described,[53] and target cells were transduced at multiplicity of infection (MOI) of 40. ETS1 overexpression in SW480-ADH cells was performed by transient transfection of exogenous ETS1 cDNA (OriGene, Rockville, MD, USA; #RG227466).

Quantitative RT-PCR

Total RNA was purified using the NucleoSpin® miRNA extraction kit (Macherey-Nagel, Düren, Germany). Quantitative real-time PCR (qRT-PCR) analyses of *SPRY2* (Hs00183386_m1), *CDH1* (Hs01023894_m1), *CLDN1* (Hs00221623_m1), *CLDN7* (Hs00600772_m1), *ESRP1* (Hs00214472_m1), *INADL* (Hs00195106_m1), *LLGL2* (Hs00189729_m1), *OCLN* (Hs00170162_m1), *ST14* (Hs01058386_m1) were performed using the TaqMan Gene Expression Master Mix (Applied Biosystems, Foster City, CA, USA). RNA expression values were normalized versus the housekeeping gene *RPLPO* (Large Ribosomal Protein). The reaction was performed in a CFX384

Real-Time PCR Detection System (Bio-Rad, Hercules, CA, USA). Quantitative real-time PCR (qRT-PCR) analyses of *hsa-miR-200b* 002251, *-200c* 002300, *-142-3p* 000464, *-23a* 000399, *-150* 000473, and *-342-3p* 002260 were performed by using miRNA-specific TaqMan MicroRNA Assay Kit (Applied Biosystems). *RNU44* 001094 small RNA was used for normalization of input RNA/cDNA levels. *ZEB1* expression was analyzed by using primers forward 5'-GCCAATAAGCAAACGATTCTG-3' and reverse 5'-TTTGGCTGGATCACTTTCAAG-3'. Values were normalized versus housekeeping gene succinate dehydrogenase complex subunit A (*SDHA*), forward 5'-TGGGAACAAGAGGGCATCTG-3' and reverse 5'-CCACCACTGCATCAAATTCATG-3'. All experiments were performed at least three times using triplicates.

Western blot

Western blot was performed as previously described.[7] Proteins were analyzed by using the Odyssey Infrared Imaging or revealed following the ECL technique (Amersham, Buckinghamshire, UK). Different exposure times of the films were used to ensure that bands were not saturated. Western blots in all figures correspond to a representative experiment of at least three performed. Quantification of the experiments is indicated in each figure.

Immunofluorescence and confocal microscopy

Tissue Microarrays (TMA) corresponding to human colorectal (CRC) tumors at Stage III, from a collection available in the Pathology Service of the Vall d´Hebron Hospital, were chosen since the protein markers evaluated could potentially have predictive value on cancer progression. Previous data in CRC indicate that the probability of SPRY2

expression is around 0.90. If the probability of SPRY2-mediated ZEB1 overexpression exposure among cases is 0.80, we will need to study 33 cases patients to be able to detect the association between SPRY2 and ZEB1, with a power of 0.90 and two-sided error of 0.05. We used an uncorrected χ^2 statistic to evaluate this hypothesis (PS Power and Sample Size Calculation v3.0). TMA were prepared and immunolabeled as described elsewhere.[54] Briefly, antigens were retrieved by microwaving in 10 mM citrate buffer (pH 6.0) for 10 min and permeabilized with 0.2% Triton X-100 (Sigma-Aldrich). Non-specific binding was blocked by incubating the sections in 10% BSA (Sigma-Aldrich) for 1 h. Cell imaging was performed on a Leica TCS SP5 DMI6000 microscope using argon ion (488 nm), HeNe (543 nm) and violet diode (405 nm) lasers. Images were acquired sequentially by direct register using Leica Confocal Software (LAS AF). Fluorescence image data were analyzed with the MBF "ImageJ for Microscopy"-program collection of plugins (www.macbiophotonics.ca), using criteria described earlier.[55] Briefly, we defined Regions of Interest (ROI) in images of immunostained tissues encompassing only tumoral tissue. First, using ImageJ software, we obtained the integrated density value and each channel-molecule (SPRY2, red channel; ZEB1 or claudin-7, green channel) and Hoechst 33342 (blue channel) for each ROI. Next, we measured the integrated density for Hoechst signal present in each ROI and normalized by a standard nucleus signal, defined as the average integrated density of ten nuclei taken at random. The resulting values correspond to the number of nuclei and, therefore, to the number of cells present in each ROI. Finally, we divided the values of the integrated density for each protein of interest (green or red channels) by the calculated number of cancer cells in the corresponding ROI. These values indicate the level of expression for each protein per cancer cell analyzed noted as relative units (r. u.) in the corresponding figures.

Gene expression analysis

Microarray analyses were performed using RNAs obtained from Mock, SPRY2-wt, SPRY2-S112A and SPRY2-Y55F cells in three independent experiments performed in triplicate. Total RNA was extracted following manufacturer's instructions (Macherey-Nagel). RNA integrity was assessed using Agilent 2100 Bioanalyzer (Agilent, Palo Alto, CA, USA). Total RNA samples were then processed for hybridization on Gene Chip Human Gene 1.0 ST Array (Affymetrix, Santa Clara, CA, USA) using standard Affymetrix protocols at the Genomics and Proteomics Facility of Centro de Investigación del Cáncer (Salamanca, Spain). Scanning was performed using GeneChip System of Affymetrix (GeneChip Hybridization Oven 640, GeneChip Fluidics Station 450 and GeneChip Scanner 7G). The Robust Microarray Analysis (RMA) algorithm was used for background correction, intra- and inter-microarray normalization, and expression signal calculation.[56] The absolute expression signal for each gene was calculated for each microarray. The expression signal was calculated using the CDF package called GeneMapper from GATExplorer (genemapperhumangene1.0cdf; see webite: http://bioinfow.dep.usal.es/xgate/ mapping/mapping.php),[57] which maps into an updated version of human genes, instead of using the original probe-set definition provided by *Affymetrix*. This mapping provides an improvement thanks to the re-annotation to updated gene loci and removal of cross-hybridation noise.[57] It also allows us to operate from the beginning using gene identification (Ensembl IDs) instead of probe sets (*Affymetrix* IDs). Mapping to genome version Ensembl v57 (assembly GRCh37) was used for these analyses.

Analysis for differential expression was performed using the R platform for statistical analysis (R Development Core Team (2010). R: A language and environment

for statistical computing. R Foundation for Statistical Computing, Vienna, Austria. ISBN 3-900051-07-0, URL http://www.R-project.org/), and several packages from the Bioconductor project[58] (http://www.bioconductor.org/). The raw data were imported into R and preprocessed using the *affy* package and the robust multichip average method. Further, Pearson correlation test and Principal Component Analysis (PCA) were carried out with all genes included in the dataset. To identify differentially expressed genes, we used the *limma* package. Correction for multiple testing was accomplished by controlling the false discovery rate (FDR) using published methods (FDR = 0.1).[59] The experimental settings and raw data obtained in this experiment are deposited in GEO (accession number GSE56941).

Functional Enrichment Analysis

Single Enrichment Analysis (SEA) was performed with differentially expressed genes between conditions. This analysis was carried out with the functional annotation tool included in the DAVID Bioinformatics Resources. We considered only pathways with a Benjamini *P* value lower than 0.05 for the Kyoto Encyclopedia of Genes and Genomes (KEGG), REACTOME, and Gene Ontology – Biological Process databases. We used Gene Set Enrichment Analysis (GSEA)[60] (www.broadinstitute.org/gsea) to assess the degree of association between our signature (expression data set) and some other signatures previously defined with genes significantly enriched in adhesion (gene sets: REACTOME Adherens_junctions_interactions, Gene Ontology: 0005911 Intercellular junctions, Gene Ontology: 0030054 Cell_junctions, KEGG Adherens junctions, KEGG tight junctions, KEGG gap junctions). GSEA requires ranking genes according to their association with a given phenotype, and determining whether genes in a signature tend to present either high (positively enriched) or low ranks (negatively enriched). The

output of GSEA is an enrichment score (ES), a normalized enrichment score (NES) which accounts for the size of the gene set being tested, a *P*-value and an estimated FDR. ES, NES and FDR were obtained as proposed previously.[60]

Statistical analysis

Statistical analysis was performed using GraphPad Instat (GraphPad Software, San Diego, CA, USA). All experiments and qRT-PCR analyses were performed at least three times using triplicates. Significant differences between groups, expressed as mean ± standard error of the mean (s.e.m), were calculated by parametric one-way ANOVA using Tukey-Kramer post-test, and correlation coefficients (*r*) were calculated by no parametric Spearman's test. Homogeneity of variances between groups was analyzed using Brown-Forsythe test (n.s. $P > 0.05$). The single asterisk indicates $P < 0.05$, the double asterisk $P < 0.01$, and the triple asterisk $P < 0.001$. $P > 0.05$ were considered not significant (n.s.).

Ethics statement

The work involving human samples was conducted according to the principles expressed in the Declaration of Helsinki. The study was approved by the Research Ethics Committee of Vall d'Hebron University Hospital (Barcelona, Spain) (Approval ID: PR(IR)79/2009). All patients provided written informed consent for the collection of samples and subsequent analysis.

CONFLICT OF INTEREST

The authors declare no conflict of interest.

ACKNOWLEDGEMENTS

We thank Drs. G. Goodall, T. Brabletz and A. García de Herreros for kindly providing us reagents, T. Martínez and X. Langa for technical assistance and Robin Rycroft for help with the English manuscript. This study was supported by the Ministerio de Economía y Competitividad of Spain and Fondo Europeo de Desarrollo Regional (FEDER) (grant SAF2013-43468-R to A.M., SAF2011-29530 to F.X.R.); FEDER-Instituto de Salud Carlos III (RD12/0036/0021 to A.M. and J.M.R., RD12/0036/0034 to F.X.R., RD12/0036/0016 to M.S., RD12/0036/0012 to H.G.P., RD06/0020/0003, PS09/00562 and PI13/00703 to J.M.R.); Comunidad de Madrid (S2010/BMD-2344 Colomics2 to A.M.); Fundación Científica de la Asociación Española contra el Cáncer (to J.M.R.); U.S. Department of Defense (CA093471 and CA110602 to E.H.); National Institutes of Health/National Cancer Institute (1R01CA155234-01 to E.H.); National Institutes of Health/National Institute of Arthritis and Musculoskeletal and Skin Diseases (1R21AR062239-01 to E.H.); and the Melanoma Research Alliance (to E. H.).

REFERENCES

1 Cabrita MA, Christofori G. Sprouty proteins, masterminds of receptor tyrosine kinase signaling. Angiogenesis 2008; 11: 53-62.

2 Masoumi-Moghaddam S, Amini A, Morris DL. The developing story of Sprouty and cancer. Cancer Metastasis Rev 2014; 33: 695-720.

3 Egan JE, Hall AB, Yatsula BA, Bar-Sagi D. The bimodal regulation of epidermal growth factor signaling by human Sprouty proteins. Proc Natl Acad Sci U S A 2002; 99: 6041-6046.

4 Rubin C, Litvak V, Medvedovsky H, Zwang Y, Lev S, Yarden Y. Sprouty fine-tunes EGF signaling through interlinked positive and negative feedback loops. Curr Biol 2003; 13: 297-307.

5 Wong ES, Fong CW, Lim J, Yusoff P, Low BC, Langdon WY *et al*. Sprouty2 attenuates epidermal growth factor receptor ubiquitylation and endocytosis, and consequently enhances Ras/ERK signalling. Embo J 2002; 21: 4796-4808.

6 Haglund K, Schmidt MH, Wong ES, Guy GR, Dikic I. Sprouty2 acts at the Cbl/CIN85 interface to inhibit epidermal growth factor receptor downregulation. EMBO Rep 2005; 6: 635-641.

7 Barbachano A, Ordonez-Moran P, Garcia JM, Sanchez A, Pereira F, Larriba MJ *et al*. SPROUTY-2 and E-cadherin regulate reciprocally and dictate colon cancer cell tumourigenicity. Oncogene 2010; 29: 4800-4813.

8 Holgren C, Dougherty U, Edwin F, Cerasi D, Taylor I, Fichera A *et al*. Sprouty-2 controls c-Met expression and metastatic potential of colon cancer cells: sprouty/c-Met upregulation in human colonic adenocarcinomas. Oncogene 2010; 29: 5241-5253.

9 Watanabe T, Kobunai T, Yamamoto Y, Matsuda K, Ishihara S, Nozawa K *et al*. Differential gene expression signatures between colorectal cancers with and without KRAS mutations: crosstalk between the KRAS pathway and other signalling pathways. Eur J Cancer 2011; 47: 1946-1954.

10 Tsavachidou D, Coleman ML, Athanasiadis G, Li S, Licht JD, Olson MF *et al*. SPRY2 is an inhibitor of the ras/extracellular signal-regulated kinase pathway in melanocytes and melanoma cells with wild-type BRAF but not with the V599E mutant. Cancer Res 2004; 64: 5556-5559.

11 Bloethner S, Chen B, Hemminki K, Muller-Berghaus J, Ugurel S, Schadendorf D *et al*. Effect of common B-RAF and N-RAS mutations on global gene expression in melanoma cell lines. Carcinogenesis 2005; 26: 1224-1232.

12 Rhodes DR, Yu J, Shanker K, Deshpande N, Varambally R, Ghosh D *et al*. ONCOMINE: a cancer microarray database and integrated data-mining platform. Neoplasia 2004; 6: 1-6.

13 Ordonez-Moran P, Irmisch A, Barbachano A, Chicote I, Tenbaum S, Landolfi S *et al*. SPROUTY2 is a beta-catenin and FOXO3a target gene indicative of poor prognosis in colon cancer. Oncogene 2014; 33: 1975-1985.

14 Feng YH, Wu CL, Tsao CJ, Chang JG, Lu PJ, Yeh KT *et al*. Deregulated expression of sprouty2 and microRNA-21 in human colon cancer: Correlation with the clinical stage of the disease. Cancer Biol Ther 2011; 11: 111-121.

15 McKie AB, Douglas DA, Olijslagers S, Graham J, Omar MM, Heer R *et al*. Epigenetic inactivation of the human sprouty2 (hSPRY2) homologue in prostate cancer. Oncogene 2005; 24: 2166-2174.

16 Fong CW, Chua MS, McKie AB, Ling SH, Mason V, Li R *et al*. Sprouty 2, an inhibitor of mitogen-activated protein kinase signaling, is down-regulated in hepatocellular carcinoma. Cancer Res 2006; 66: 2048-2058.

17 Sánchez A, Setien F, Martínez N, Oliva JL, Herranz M, Fraga MF *et al*. Epigenetic inactivation of the ERK inhibitor Spry2 in B-cell diffuse lymphomas. Oncogene 2008; 27: 4969-4972.

18 Frank MJ, Dawson DW, Bensinger SJ, Hong JS, Knosp WM, Xu L *et al*. Expression of sprouty2 inhibits B-cell proliferation and is epigenetically silenced in mouse and human B-cell lymphomas. Blood 2009; 113: 2478-2487.

19 Faratian D, Sims AH, Mullen P, Kay C, Um I, Langdon SP *et al*. Sprouty 2 is an independent prognostic factor in breast cancer and may be useful in stratifying patients for trastuzumab therapy. PLoS One 2011; 6: e23772.

20 Buzza MS, Netzel-Arnett S, Shea-Donohue T, Zhao A, Lin CY, List K *et al*. Membrane-anchored serine protease matriptase regulates epithelial barrier formation and permeability in the intestine. Proc Natl Acad Sci U S A 2010; 107: 4200-4205.

21 Guy GR, Wong ES, Yusoff P, Chandramouli S, Lo TL, Lim J *et al*. Sprouty: how does the branch manager work? J Cell Sci 2003; 116: 3061-3068.

22 Li X, Brunton VG, Burgar HR, Wheldon LM, Heath JK. FRS2-dependent SRC activation is required for fibroblast growth factor receptor-induced phosphorylation of Sprouty and suppression of ERK activity. J Cell Sci 2004; 117: 6007-6017.

23 DaSilva J, Xu L, Kim HJ, Miller WT, Bar-Sagi D. Regulation of sprouty stability by Mnk1-dependent phosphorylation. Molecular and cellular biology 2006; 26: 1898-1907.

24 Edwin F, Anderson K, Patel TB. HECT domain-containing E3 ubiquitin ligase Nedd4 interacts with and ubiquitinates Sprouty2. J Biol Chem 2010; 285: 255-264.

25 Dhawan P, Singh AB, Deane NG, No Y, Shiou S-R, Schmidt C *et al*. Claudin-1 regulates cellular transformation and metastatic behavior in colon cancer. J Clin Invest 2005; 115: 1765-1776.

26 Lee M, Vasioukhin V. Cell polarity and cancer--cell and tissue polarity as a non-canonical tumor suppressor. J Cell Sci 2008; 121: 1141-1150.

27 Spaderna S, Schmalhofer O, Wahlbuhl M, Dimmler A, Bauer K, Sultan A *et al*. The transcriptional repressor ZEB1 promotes metastasis and loss of cell polarity in cancer. Cancer Res 2008; 68: 537-544.

28 List K, Kosa P, Szabo R, Bey AL, Wang CB, Molinolo A *et al*. Epithelial integrity is maintained by a matriptase-dependent proteolytic pathway. Am J Pathol 2009; 175: 1453-1463.

29 van der Gun BT, Huisman C, Stolzenburg S, Kazemier HG, Ruiters MH, Blancafort P *et al*. Bidirectional modulation of endogenous EpCAM expression to unravel its function in ovarian cancer. British journal of cancer 2013; 108: 881-886.

30 Lei Z, Maeda T, Tamura A, Nakamura T, Yamazaki Y, Shiratori H *et al*. EpCAM contributes to formation of functional tight junction in the intestinal epithelium by recruiting claudin proteins. Dev Biol 2012; 371: 136-145.

31 Wu CJ, Mannan P, Lu M, Udey MC. Epithelial cell adhesion molecule (EpCAM) regulates claudin dynamics and tight junctions. J Biol Chem 2013; 288: 12253-12268.

32 Brown RL, Reinke LM, Damerow MS, Perez D, Chodosh LA, Yang J *et al*. CD44 splice isoform switching in human and mouse epithelium is essential for epithelial-mesenchymal transition and breast cancer progression. J Clin Invest 2011; 121: 1064-1074.

33 Warzecha CC, Carstens RP. Complex changes in alternative pre-mRNA splicing play a central role in the epithelial-to-mesenchymal transition (EMT). Semin Cancer Biol 2012; 22: 417-427.

34 Gemmill RM, Roche J, Potiron VA, Nasarre P, Mitas M, Coldren CD *et al*. ZEB1-responsive genes in non-small cell lung cancer. Cancer Lett 2011; 300: 66-78.

35 Horiguchi K, Sakamoto K, Koinuma D, Semba K, Inoue A, Inoue S *et al*. TGF-beta drives epithelial-mesenchymal transition through deltaEF1-mediated downregulation of ESRP. Oncogene 2012; 31: 3190-3201.

36 Aigner K, Dampier B, Descovich L, Mikula M, Sultan A, Schreiber M *et al*. The transcription factor ZEB1 (deltaEF1) promotes tumour cell dedifferentiation by repressing master regulators of epithelial polarity. Oncogene 2007; 26: 6979-6988.

37 Gregory PA, Bert AG, Paterson EL, Barry SC, Tsykin A, Farshid G *et al*. The miR-200 family and miR-205 regulate epithelial to mesenchymal transition by targeting ZEB1 and SIP1. Nat Cell Biol 2008; 10: 593-601.

38 Korpal M, Lee ES, Hu G, Kang Y. The miR-200 family inhibits epithelial-mesenchymal transition and cancer cell migration by direct targeting of E-cadherin transcriptional repressors ZEB1 and ZEB2. J Biol Chem 2008; 283: 14910-14914.

39 Burk U, Schubert J, Wellner U, Schmalhofer O, Vincan E, Spaderna S *et al*. A reciprocal repression between ZEB1 and members of the miR-200 family promotes EMT and invasion in cancer cells. EMBO Rep 2008; 9: 582-589.

40 Bracken CP, Gregory PA, Kolesnikoff N, Bert AG, Wang J, Shannon MF *et al*. A double-negative feedback loop between ZEB1-SIP1 and the microRNA-200 family regulates epithelial-mesenchymal transition. Cancer Res 2008; 68: 7846-7854.

41 Ozaki K, Miyazaki S, Tanimura S, Kohno M. Efficient suppression of FGF-2-induced ERK activation by the cooperative interaction among mammalian Sprouty isoforms. J Cell Sci 2005; 118: 5861-5871.

42 Dave N, Guaita-Esteruelas S, Gutarra S, Frias A, Beltran M, Peiro S *et al*. Functional cooperation between Snail1 and twist in the regulation of ZEB1 expression during epithelial to mesenchymal transition. J Biol Chem 2011; 286: 12024-12032.

43 Martin-Belmonte F, Perez-Moreno M. Epithelial cell polarity, stem cells and cancer. Nat Rev Cancer 2012; 12: 23-38.

44 Bornholdt J, Friis S, Godiksen S, Poulsen SS, Santoni-Rugiu E, Bisgaard HC *et al*. The level of claudin-7 is reduced as an early event in colorectal carcinogenesis. BMC Cancer 2011; 11: 65.

45 Darido C, Buchert M, Pannequin J, Bastide P, Zalzali H, Mantamadiotis T *et al*. Defective claudin-7 regulation by Tcf-4 and Sox-9 disrupts the polarity and increases the tumorigenicity of colorectal cancer cells. Cancer Res 2008; 68: 4258-4268.

46 Nakayama F, Semba S, Usami Y, Chiba H, Sawada N, Yokozaki H. Hypermethylation-modulated downregulation of claudin-7 expression promotes the progression of colorectal carcinoma. Pathobiology 2008; 75: 177-185.

47 Merikallio H, Kaarteenaho R, Paakko P, Lehtonen S, Hirvikoski P, Makitaro R *et al*. Zeb1 and twist are more commonly expressed in metastatic than primary lung tumours and show inverse associations with claudins. J Clin Pathol 2011; 64: 136-140.

48 Swat A, Dolado I, Rojas JM, Nebreda AR. Cell density-dependent inhibition of epidermal growth factor receptor signaling by p38alpha mitogen-activated

protein kinase via Sprouty2 downregulation. Molecular and cellular biology 2009; 29: 3332-3343.

49 Ono H, Imoto I, Kozaki K, Tsuda H, Matsui T, Kurasawa Y *et al*. SIX1 promotes epithelial-mesenchymal transition in colorectal cancer through ZEB1 activation. Oncogene 2012; 31: 4923-4934.

50 de Alvaro C, Martinez N, Rojas JM, Lorenzo M. Sprouty-2 overexpression in C2C12 cells confers myogenic differentiation properties in the presence of FGF2. Mol Biol Cell 2005; 16: 4454-4461.

51 Kohno Y, Okamoto T, Ishibe T, Nagayama S, Shima Y, Nishijo K *et al*. Expression of claudin7 is tightly associated with epithelial structures in synovial sarcomas and regulated by an Ets family transcription factor, ELF3. J Biol Chem 2006; 281: 38941-38950.

52 Aguilera O, Pena C, Garcia JM, Larriba MJ, Ordonez-Moran P, Navarro D *et al*. The Wnt antagonist DICKKOPF-1 gene is induced by 1alpha,25-dihydroxyvitamin D3 associated to the differentiation of human colon cancer cells. Carcinogenesis 2007; 28: 1877-1884.

53 Punzon I, Criado LM, Serrano A, Serrano F, Bernad A. Highly efficient lentiviral-mediated human cytokine transgenesis on the NOD/scid background. Blood 2004; 103: 580-582.

54 Silva-Vargas V, Lo Celso C, Giangreco A, Ofstad T, Prowse DM, Braun KM *et al*. Beta-catenin and Hedgehog signal strength can specify number and location of hair follicles in adult epidermis without recruitment of bulge stem cells. Developmental cell 2005; 9: 121-131.

55 Tenbaum SP, Ordonez-Moran P, Puig I, Chicote I, Arques O, Landolfi S *et al*. beta-catenin confers resistance to PI3K and AKT inhibitors and subverts FOXO3a to promote metastasis in colon cancer. Nature medicine 2012; 18: 892-901.

56 Irizarry RA, Hobbs B, Collin F, Beazer-Barclay YD, Antonellis KJ, Scherf U *et al*. Exploration, normalization, and summaries of high density oligonucleotide array probe level data. Biostatistics 2003; 4: 249-264.

57 Risueno A, Fontanillo C, Dinger ME, De Las Rivas J. GATExplorer: genomic and transcriptomic explorer; mapping expression probes to gene loci, transcripts, exons and ncRNAs. BMC bioinformatics 2010; 11: 221.

58 Gentleman RC, Carey VJ, Bates DM, Bolstad B, Dettling M, Dudoit S *et al*. Bioconductor: open software development for computational biology and bioinformatics. Genome biology 2004; 5: R80.

59 Benjamini Y, Drai D, Elmer G, Kafkafi N, Golani I. Controlling the false discovery rate in behavior genetics research. Behavioural brain research 2001; 125: 279-284.

60 Subramanian A, Tamayo P, Mootha VK, Mukherjee S, Ebert BL, Gillette MA *et al*. Gene set enrichment analysis: a knowledge-based approach for interpreting genome-wide expression profiles. Proc Natl Acad Sci U S A 2005; 102: 15545-15550.

FIGURE LEGENDS

Figure 1. SPRY2 represses epithelial adhesion and polarity genes. (**a**) Left, phase-contrast images of Mock, SPRY2-wt, SPRY2-S112A and SPRY2-Y55F cells. Scale bar, 50 μm. Right, Western blot analysis of the expression of the AU5-tagged SPRY2 proteins. Lamin B was used as loading control. (**b**) Quantitative RT-PCR analysis of *CDH1*, *CLDN7*, *OCLN*, *CLDN1* and *ZEB1* RNA levels, and (**c**) Western blot of ZEB1, E-cadherin, claudin-7, claudin-1 and occludin proteins in Mock, SPRY2-wt, SPRY2-S112A and SPRY2-Y55F cells. (**d**) Quantitative RT-PCR analysis of *ESRP1*, *ST14*, *INADL*, *LLGL2* and *EPCAM* RNA levels, and **(e)** Western blot of ST14 and EpCAM proteins in Mock, SPRY2-wt, SPRY2-S112A and SPRY2-Y55F cells. (**f**) Reporter assay in Mock and SPRY2-wt cells co-transfected with plasmids encoding a fragment (-1136/+428 bp) of the *CLDN7* gene upstream the luciferase cDNA or empty vector (pGL3) and *ZEB1* cDNA or empty vector (pCDNA3). The graph shows the corrected luciferase activity values represented as fold change over the activity obtained in cells transfected with *CLDN7* empty vector (pGL3) ($n = 3$).

Figure 2. Mock- and SPRY2-S112A-cell signature predicts cellular adhesion *versus* SPRY2-wt signature. Genes are ranked according to their differential expression between Mock *versus* SPRY2-wt cells (left), SPRY2-S112A *versus* SPRY2-wt cells (middle), Mock *versus* SPRY2-S112A cells (right). Gene set enrichment analysis (GSEA) results for the enrichment of this gene set (GEO accession: GSE56941) detected toward the data sets: *adherens* junctions (KEGG pathways), intercellular junctions (Gene Ontology (GO): 0005911) and cell-to cell and extracellular matrix junctions as "cell junctions" (GO: 0030054). Black bars below the graph depict the

position of genes significantly enriched. ES, enrichment score; NES, normalized enrichment score; FDR, false discovery rate. NS, not significant.

Figure 3. *ZEB1* knock-down has opposite effects than *SPRY2* expression on cell adhesion and polarity genes. (**a**) Quantitative RT-PCR analysis of RNA and **(b)** Western blot analysis of several adhesion and polarity genes/proteins in Mock cells transfected with control (non-silencing, NS; Mock-NS) or *ZEB1* shRNA (pool and clone #7). (**c**) Quantitative RT-PCR analysis of *miR-200b* and *miR-200c* expression in Mock-NS or *ZEB1* shRNA cells. (**d**) Quantitative RT-PCR analysis of RNA and (**e**) Western blot analysis of adhesion and polarity genes/proteins in SPRY2-wt cells transduced with NS or three different *ZEB1* shRNA lentivirus (sh1, sh2 and sh3). (**f**) Quantitative RT-PCR analysis of *miR-200b* and *miR-200c* expression in SPRY2-wt transduced with NS or *ZEB1* shRNA. (**g**) Reporter assay in control (NS) and *ZEB1* knocked-down (sh1 and sh2) SPRY2-wt cells transfected with *CLDN7*, *CDH1* promoters and empty plasmid pGL3. Graphs show corrected luciferase activity values represented as fold change over the activity obtained in cells transfected with empty vector (pGL3) ($n = 3$).

Figure 4. SPRY2 expression correlates directly with that of ZEB1 and inversely with that of claudin-7 in human colon tumors. (**a**) Representative images showing protein expression by double immunofluorescence and confocal microscopy of ZEB1 (green), and claudin-7 (green) in patients with high (patient 1) or low (patient 2) SPRY2 expression (red). Nuclei were stained with Hoechst 33342 (blue). Scale bars: 100 μm. (**b**) Scatter plots showing the corresponding intensity correlation analyses of SPRY2 *vs*

ZEB1 (left), ZEB1 *vs* claudin-7 (middle) and SPRY2 *vs* claudin-7 (right). Statistical analysis was determined by non-parametric Spearman's test.

Figure 5. Repression of *miR*-200 and other *miR* species by SPRY2. (**a**) Putative binding sites for evolutionarily conserved *miR* species predicted by *in silico* analysis of *ZEB1*-RNA-3'UTR region using TargetScan, miRANDA and PicTar algorithms. Venn diagram showing common sites found. (**b**) Quantitative RT-PCR analysis of expression level of the indicated *miRs* in Mock (white columns) and SPRY2-wt (black columns) cells. *miR-RNU-44* was used as internal control (all panels). (**c**) RNA levels of *miR-200b* and *miR-200c* in Mock and SPRY2-wt, SPRY2-S112A and SPRY2-Y55F cells. (**d**) Reporter assay of HEK293T cells co-transfected with a *ZEB1*-RNA-3'UTR luciferase plasmid construct and mimic oligonucleotides (white columns, 5 nM; black columns, 50 nM) of *miR-200b, miR-142-3p, miR-23a, miR-150,* or a negative control (scrambled, Scr) (n = 3). (**e**) Left, description of wild-type and mutated binding sequences for *miR* species in *ZEB1*-RNA-3'UTR used in the following studies. Right, reporter assay of HEK293T cells co-transfected with a plasmid containing *ZEB1*-RNA-3'UTR luciferase construct mutated in the predicted sites for *miR-200* family, *miR-150* or *miR-142-3p*, and with mimic oligonucleotides of *miR-200b, miR-142-3p, miR-150* or Scr (n = 3). (**f**) Quantitative RT-PCR analysis of *ZEB1* RNA levels in Mock and SPRY2-wt cells that were transfected with mimic oligonucleotides of *miR-200b, miR-142-3p, miR-150, miR23a* or Scr. (**g**) Western blot analysis of the expression of ZEB1, E-cadherin, and claudin-7 proteins in Mock and SPRY2-wt cells that were transfected with mimic oligonucleotides of *miR-200b, miR-150, miR-142-3p, miR23a* or Scr. AU5 and Lamin B were used as control. (**h**) Activity of the *miR-200c* (-683/-67) and *miR-200b/a* (-321/+120) promoters in Mock and SPRY2-wt cells transfected with plasmids

expressing ZEB1 or an empty vector (pCDNA3) (n = 3). (**i**) Left, activity of the *miR-200c* and *miR-200b/a* promoters in SW480-ADH cells transiently transfected with expression plasmids for SPRY2 and ZEB1 or their empty vector (pCDNA3) (n = 3). Right, Western blot analysis of ZEB1 protein in transfected cells. In reporter assays, graphs show corrected luciferase activity values represented as fold change over the activity obtained in cells transfected with control vector of *miR-200c* and *miR-200b/a* (pGL3).

Figure 6. Mechanism of SPRY2 action. (**a**) Western blot analysis (left) and quantification (right, n = 3) of phospho(p)-ERK proteins normalized to total ERK in serum-starved (overnight) Mock and SPRY2-wt cells at different times of treatment with 100 ng/mL EGF (+) or vehicle (-).Lamin B protein was used as loading control. (**b**) Western blot analysis of p-AKT in serum-starved Mock and SPRY2-wt cells at different times of treatment with 100 ng/mL EGF (+) or vehicle (-). (**c**) Western blot analysis of ZEB1, p-AKT and p-S6 proteins in SPRY2-wt cells treated with increasing doses of wortmannin or MK2266 for 24 h. Total AKT, S6, lamin B and AU5 antibodies were used as controls. (**d**) Western blot analysis (left) of ZEB1, E-cadherin and claudin-7 proteins in Mock and SPRY2-wt cells treated with 5 μM PP2A (+) or vehicle (-) for 24 h (left), and quantification of ZEB1 expression (n = 4) (right). (**e**) Western blot analysis of ETS1 protein in Mock, SPRY2-wt, SPRY2-S112A and SPRY2-Y55F cells. (**f**) Western blot analysis of ETS1 and ZEB1 proteins in Mock and SPRY2-wt transduced with two different shRNA lentiviruses for *ETS1* (sh1 and sh2) and control (NS). (**g**) Western blot analysis of ETS1 and ZEB1 proteins in Mock and SPRY2-wt cells after ZEB1 silencing (sh1 and sh2). (**h**) Western blot analysis of ETS1 and ZEB1 proteins in SW480-ADH cells transiently transfected with and expression vector for human *ETS1*

cDNA. Lamin B was used as loading control. (**i**) Scheme of the mechanism of action of SPRY2 in colon carcinoma cells.

Figure 1

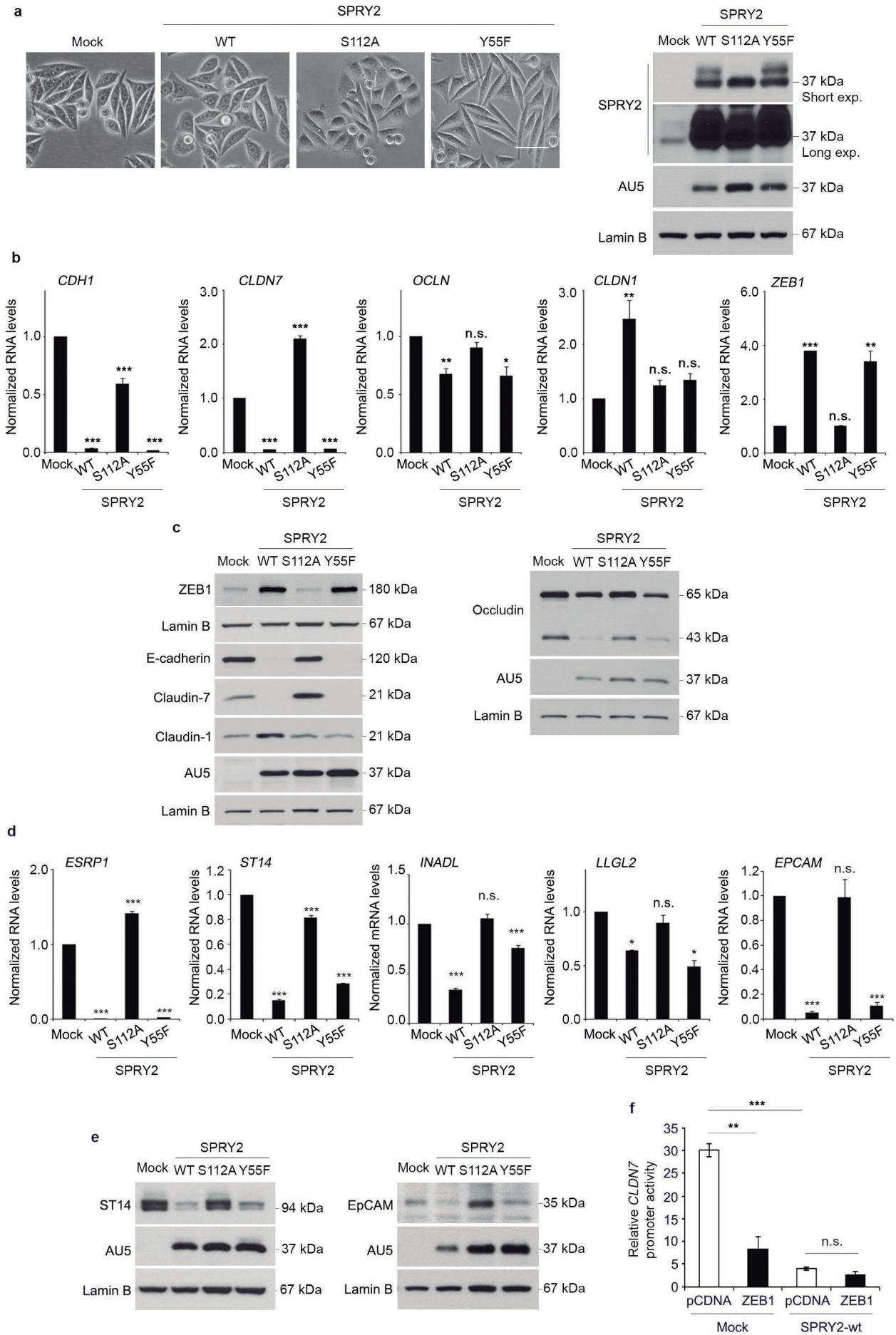
a
SPRY2
Mock
WT
S112A
Y55F
Mock WT S112A Y55F
SPRY2
37 kDa
Short exp.
37 kDa
Long exp.
AU5
37 kDa
Lamin B
67 kDa
b
CDH1
CLDN7
OCLN
CLDN1
ZEB1
Normalized RNA levels
n.s.
c
ZEB1
180 kDa
Lamin B
67 kDa
E-cadherin
120 kDa
Claudin-7
21 kDa
Claudin-1
21 kDa
AU5
37 kDa
Occludin
65 kDa
43 kDa
d
ESRP1
ST14
INADL
LLGL2
EPCAM
Normalized mRNA levels
e
94 kDa
EpCAM
35 kDa
f
Relative CLDN7 promoter activity
pCDNA
ZEB1
Mock
SPRY2-wt

Figure 2

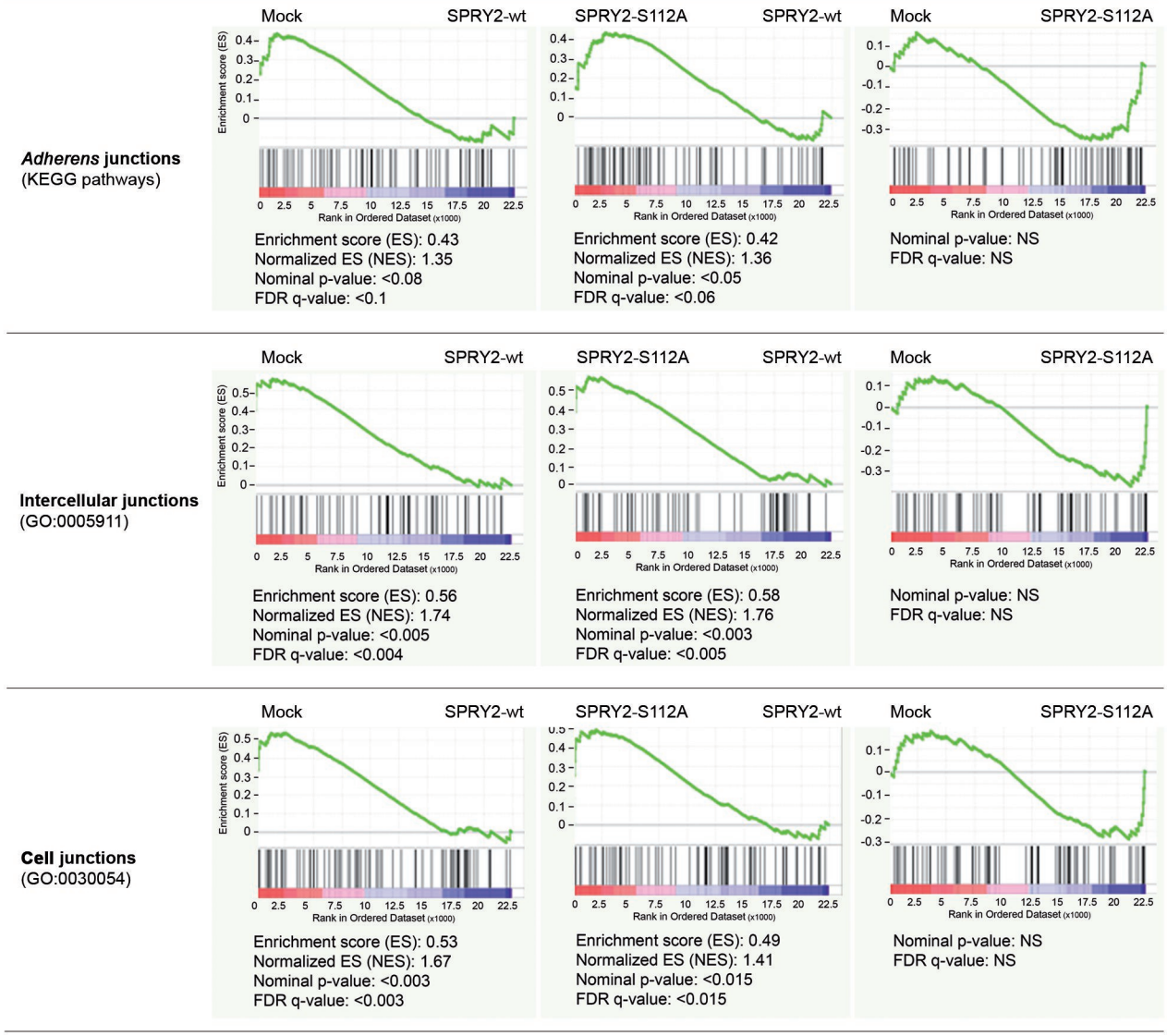
Mock
SPRY2-wt
SPRY2-S112A
SPRY2-wt
Mock
SPRY2-S112A
Enrichment score (ES)
Rank in Ordered Dataset (x1000)
Adherens junctions
(KEGG pathways)
Enrichment score (ES): 0.43
Normalized ES (NES): 1.35
Nominal p-value: <0.08
FDR q-value: <0.1
Enrichment score (ES): 0.42
Normalized ES (NES): 1.36
Nominal p-value: <0.05
FDR q-value: <0.06
Nominal p-value: NS
FDR q-value: NS
Intercellular junctions
(GO:0005911)
Enrichment score (ES): 0.56
Normalized ES (NES): 1.74
Nominal p-value: <0.005
FDR q-value: <0.004
Enrichment score (ES): 0.58
Normalized ES (NES): 1.76
Nominal p-value: <0.003
FDR q-value: <0.005
Nominal p-value: NS
FDR q-value: NS
Cell junctions
(GO:0030054)
Enrichment score (ES): 0.53
Normalized ES (NES): 1.67
Nominal p-value: <0.003
FDR q-value: <0.003
Enrichment score (ES): 0.49
Normalized ES (NES): 1.41
Nominal p-value: <0.015
FDR q-value: <0.015
Nominal p-value: NS
FDR q-value: NS

Figure 3

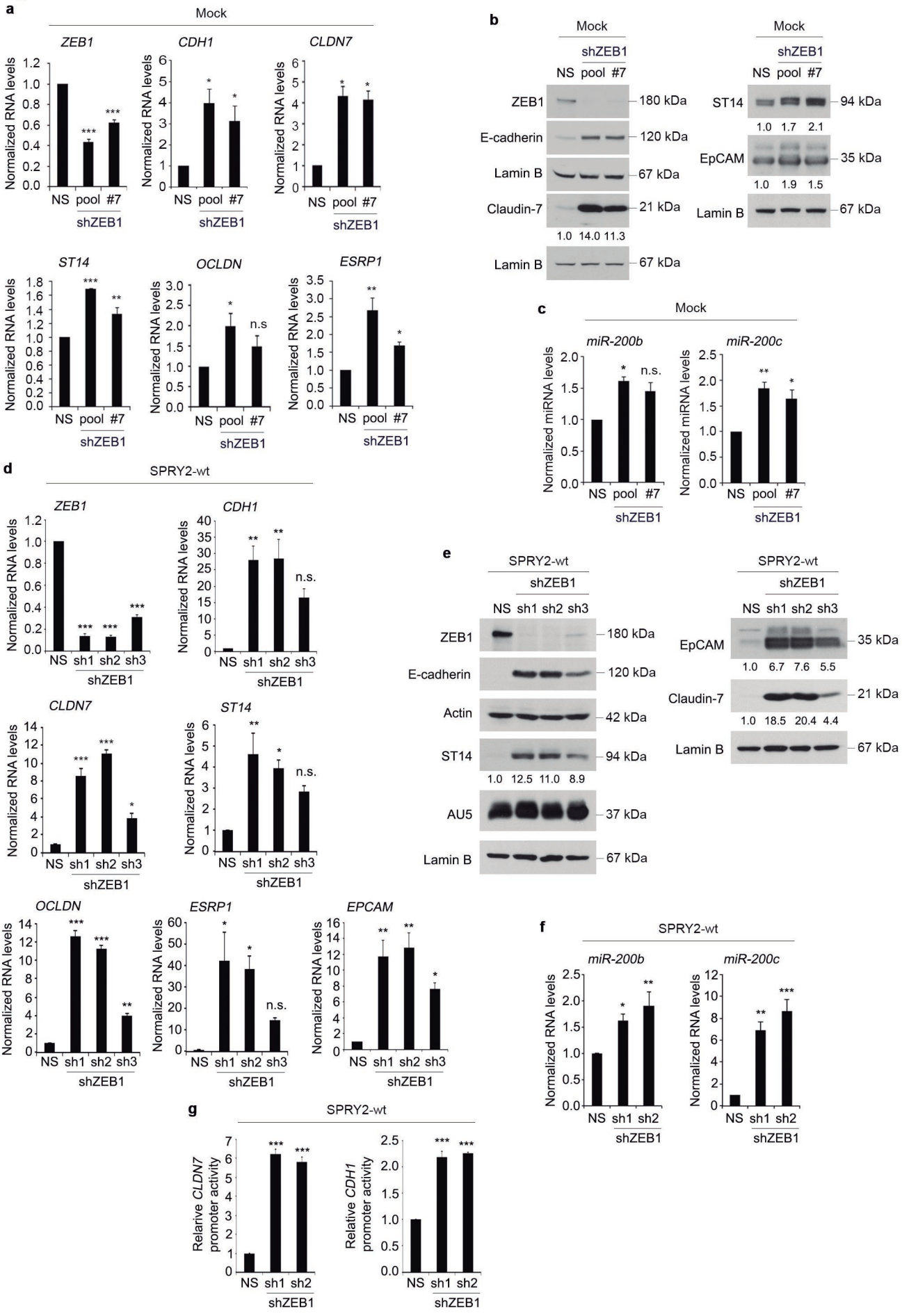
a
Mock
ZEB1
CDH1
CLDN7
ST14
OCLDN
ESRP1
Normalized RNA levels
NS pool #7
shZEB1
b
Mock
shZEB1
NS pool #7
ZEB1
E-cadherin
Lamin B
Claudin-7
ST14
EpCAM
180 kDa
120 kDa
67 kDa
21 kDa
94 kDa
35 kDa
1.0 14.0 11.3
1.0 1.7 2.1
1.0 1.9 1.5
c
Mock
miR-200b
miR-200c
Normalized miRNA levels
d
SPRY2-wt
NS sh1 sh2 sh3
e
SPRY2-wt
Actin
AU5
42 kDa
37 kDa
1.0 12.5 11.0 8.9
1.0 6.7 7.6 5.5
1.0 18.5 20.4 4.4
f
SPRY2-wt
g
SPRY2-wt
Relarive CLDN7 promoter activity
Relative CDH1 promoter activity
n.s.

Figure 4

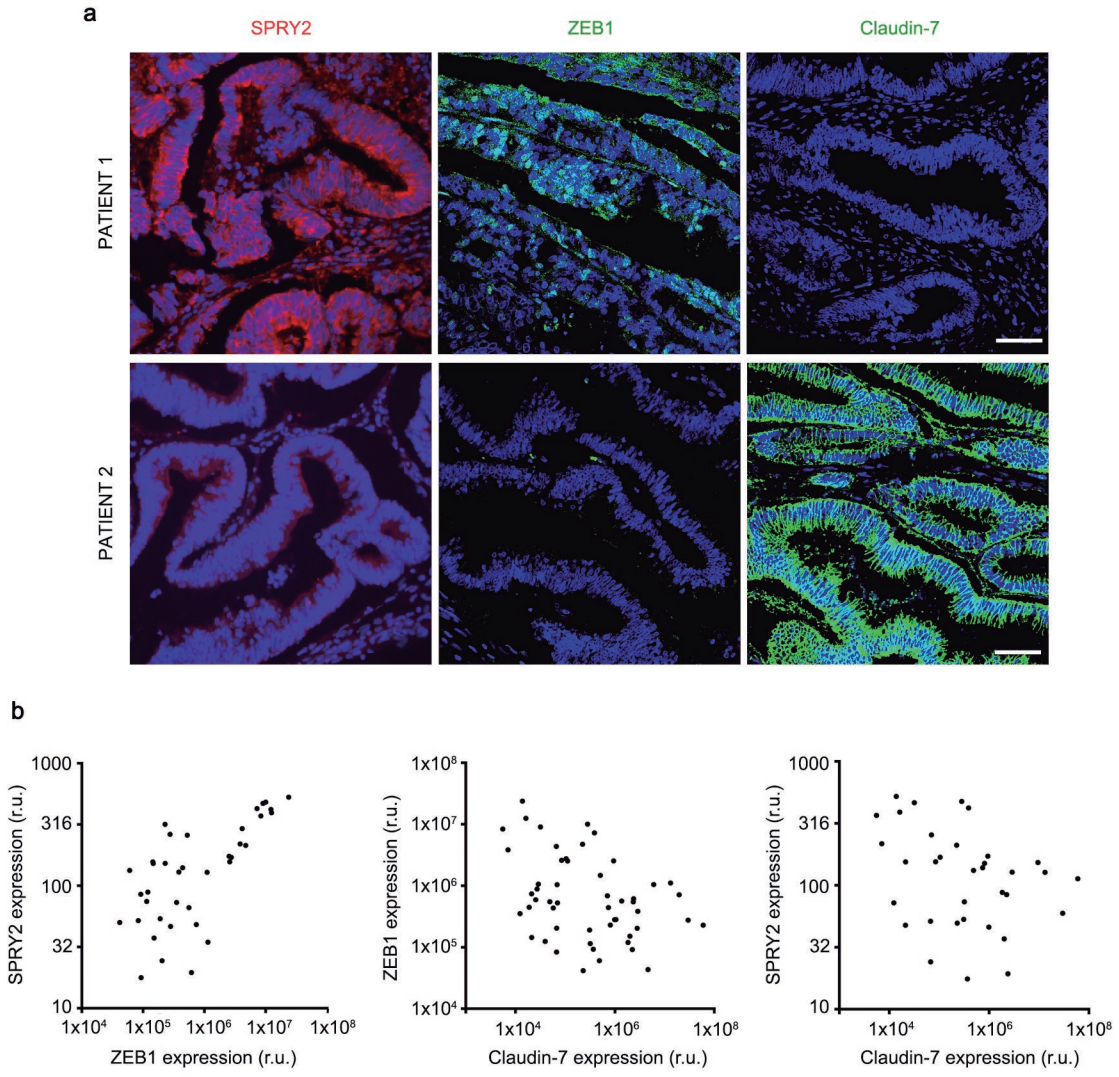
a
SPRY2
ZEB1
Claudin-7
PATIENT 1
PATIENT 2
b
SPRY2 expression (r.u.)
1000
316
100
32
10
1x10⁴
1x10⁵
1x10⁶
1x10⁷
1x10⁸
ZEB1 expression (r.u.)
ZEB1 expression (r.u.)
Claudin-7 expression (r.u.)
SPRY2 expression (r.u.)
Claudin-7 expression (r.u.)

Figure 5

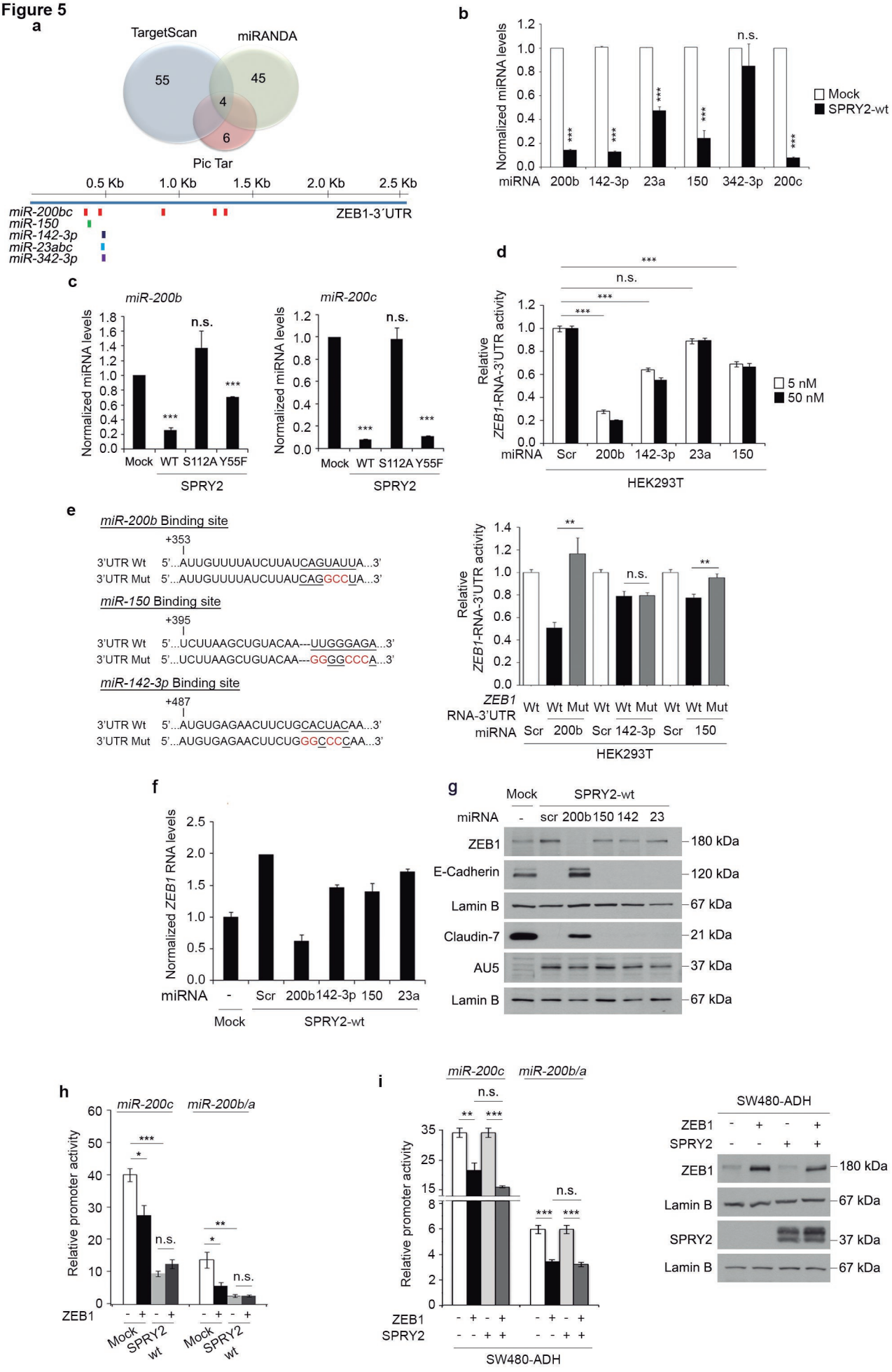
a
TargetScan
miRANDA
55
45
4
6
Pic Tar
0.5 Kb
1.0 Kb
1.5 Kb
2.0 Kb
2.5 Kb
miR-200bc
miR-150
miR-142-3p
miR-23abc
miR-342-3p
ZEB1-3´UTR
b
Normalized miRNA levels
n.s.
Mock
SPRY2-wt
miRNA 200b 142-3p 23a 150 342-3p 200c
c
miR-200b
miR-200c
Normalized miRNA levels
n.s.
Mock WT S112A Y55F
SPRY2
d
Relative ZEB1-RNA-3'UTR activity
n.s.
5 nM
50 nM
miRNA Scr 200b 142-3p 23a 150
HEK293T
e
miR-200b Binding site
+353
3'UTR Wt 5'...AUUGUUUUAUCUUAUCAGUAUUA...3'
3'UTR Mut 5'...AUUGUUUUAUCUUAUCAGGCCUA...3'
miR-150 Binding site
+395
3'UTR Wt 5'...UCUUAAGCUGUACAA---UUGGGAGA...3'
3'UTR Mut 5'...UCUUAAGCUGUACAA---GGGGCCCA...3'
miR-142-3p Binding site
+487
3'UTR Wt 5'...AUGUGAGAACUUCUGCACUACAA...3'
3'UTR Mut 5'...AUGUGAGAACUUCUGGGCCCAA...3'
Relative ZEB1-RNA-3'UTR activity
ZEB1 RNA-3'UTR
Wt Wt Mut Wt Wt Mut Wt Wt Mut
miRNA Scr 200b Scr 142-3p Scr 150
HEK293T
f
Normalized ZEB1 RNA levels
miRNA - Scr 200b 142-3p 150 23a
Mock
SPRY2-wt
g
Mock
SPRY2-wt
miRNA - scr 200b 150 142 23
ZEB1 180 kDa
E-Cadherin 120 kDa
Lamin B 67 kDa
Claudin-7 21 kDa
AU5 37 kDa
Lamin B 67 kDa
h
miR-200c
miR-200b/a
Relative promoter activity
ZEB1
Mock
SPRY2 wt
i
miR-200c
miR-200b/a
Relative promoter activity
ZEB1
SPRY2
SW480-ADH
SW480-ADH
ZEB1 180 kDa
Lamin B 67 kDa
SPRY2 37 kDa
Lamin B 67 kDa

Figure 6

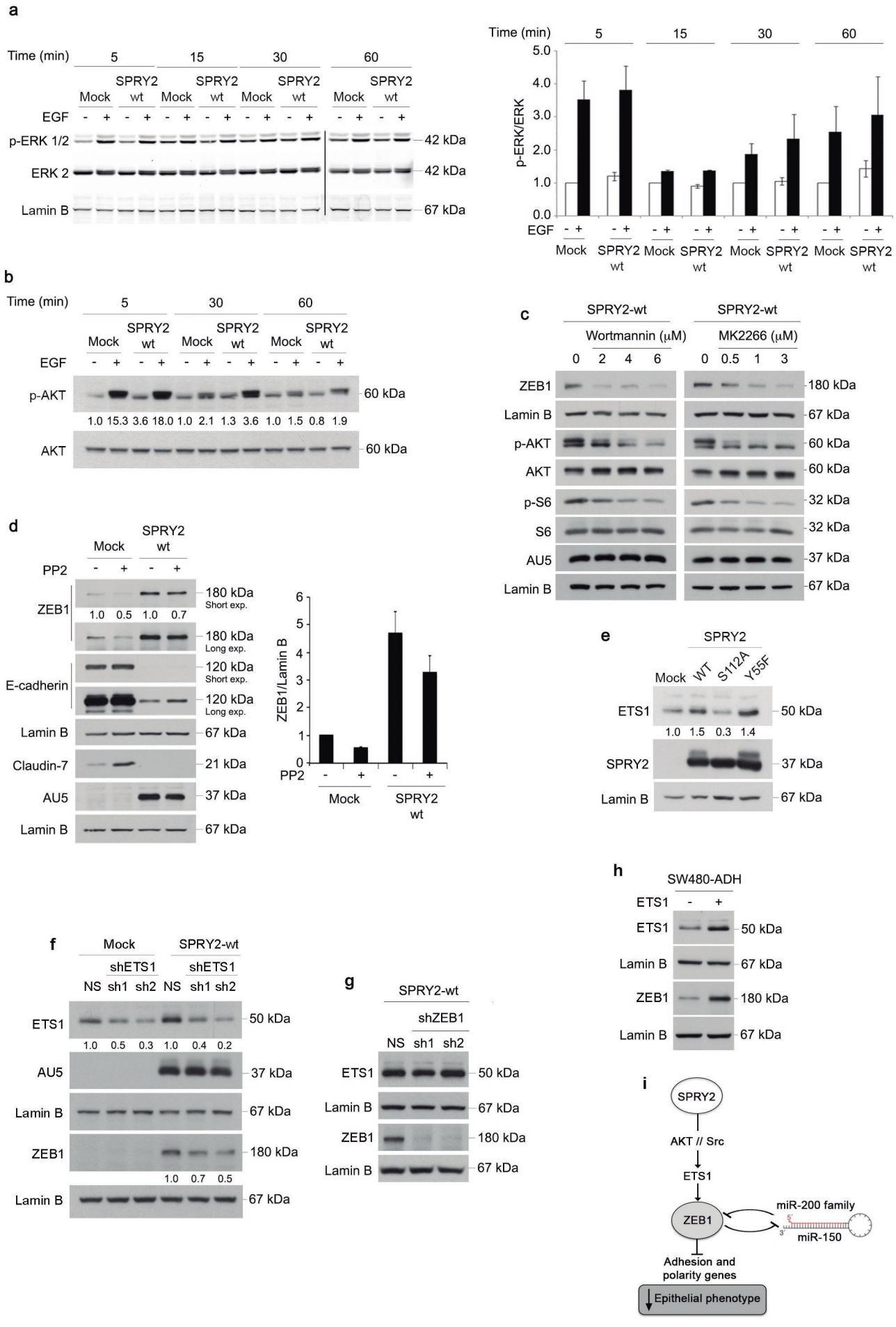
a
Time (min)
5
15
30
60
SPRY2
Mock
wt
EGF
p-ERK 1/2
ERK 2
Lamin B
42 kDa
67 kDa
p-ERK/ERK
b
p-AKT
AKT
60 kDa
1.0 15.3 3.6 18.0 1.0 2.1 1.3 3.6 1.0 1.5 0.8 1.9
c
SPRY2-wt
Wortmannin (μM)
MK2266 (μM)
ZEB1
Lamin B
p-AKT
AKT
p-S6
S6
AU5
180 kDa
32 kDa
37 kDa
d
PP2
Short exp.
Long exp.
E-cadherin
Claudin-7
1.0 0.5 1.0 0.7
ZEB1/Lamin B
e
ETS1
1.0 1.5 0.3 1.4
f
shETS1
NS sh1 sh2
1.0 0.5 0.3 1.0 0.4 0.2
1.0 0.7 0.5
g
shZEB1
h
SW480-ADH
i
SPRY2
AKT // Src
ETS1
ZEB1
miR-200 family
miR-150
Adhesion and
polarity genes
Epithelial phenotype

Supplementary Figure S1

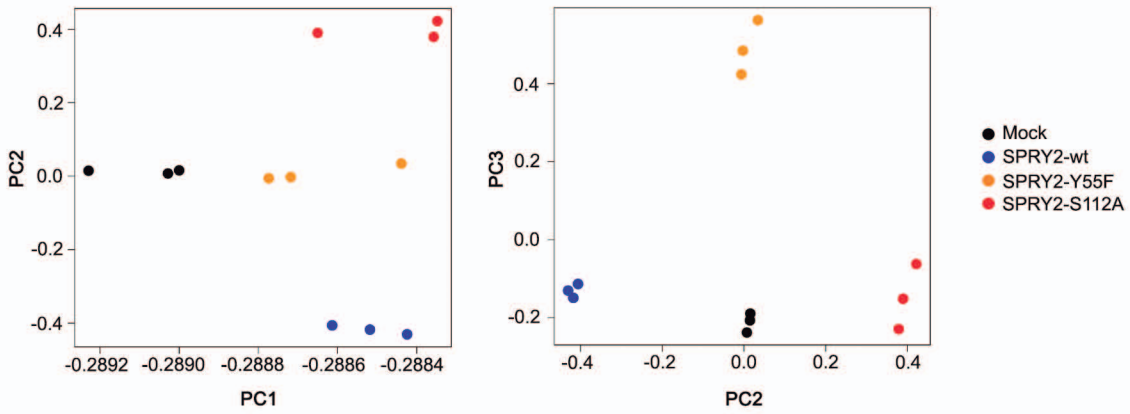

Supplementary Figure S1: Principal Component Analysis (PCA) of the global expression. Each dot represents a sample. The first three components explain the 99,7% of the variance between the samples. Left pannel: PCA plot of components 1 (importance of component - 99.25%) and 2 (0.298%); Right pannel: PCA plot of components 2 (0.298%) and 3 (0.199%).

Supplementary Figure S2

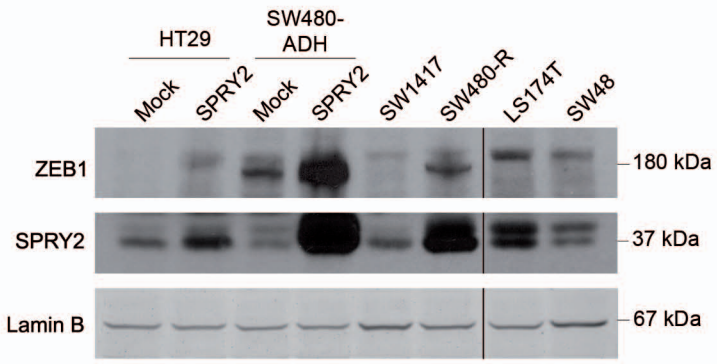

Supplementary Figure S2: Western blot analysis of ZEB1 and SPRY2 protein levels in colon carcinoma cell lines. Lamin B was used as loading control.

Supplementary Figure S3

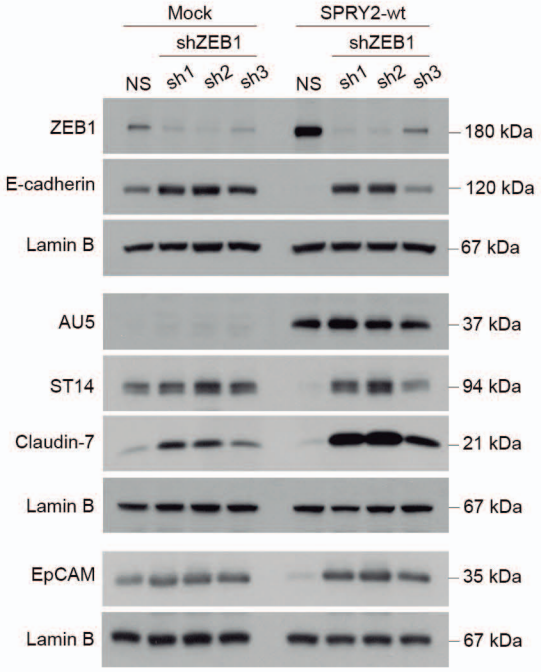

Supplementary Figure S3: Western blot analysis of adhesion and polarity proteins in Mock and SPRY2-wt cells transduced with three different *ZEB1* shRNA lentiviruses (sh1, sh2 and sh3) or a control (NS) lentivirus. Lamin B was used as loading control.

Supplementary Figure S4

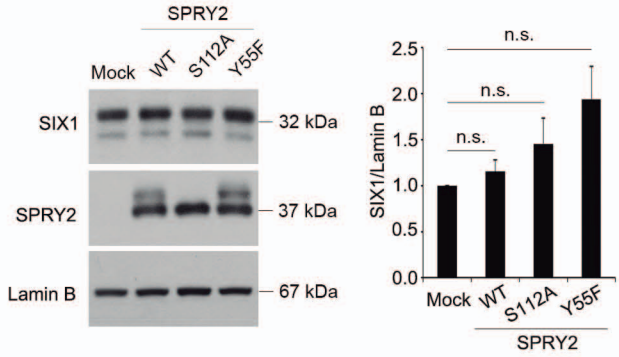

Supplementary Figure S4: Western blot analysis (left) and quantification (right) of SIX1 and SPRY2 protein levels in Mock, SPRY2-wt, SPRY2-S112A and SPRY2-Y55F cells. Lamin B was used as loading control. Bars represent mean +/- s.e.m.